Molecules and Cells

MicroRNA 449c Mediates the Generation of Monocytic Myeloid-Derived Suppressor Cells by Targeting STAT6

Xiaoqing Han, Tao Luan, Yingying Sun, Wenyi Yan, Dake Wang, and Xianlu Zeng*

The Key Laboratory of Molecular Epigenetics of Ministry of Education, Institute of Genetics and Cytology, School of Life Sciences, Northeast Normal University, Changchun 130024, China
*Correspondence: zengx779@nenu.edu.cn
https://doi.org/10.14348/molcells.2020.2307
www.molcells.org

Myeloid-derived suppressor cells (MDSCs) promote tumour progression by contributing to angiogenesis, immunosuppression, and immunotherapy resistance. Although recent studies have shown that microRNAs (miRNAs) can promote the expansion of MDSCs in the tumour environment, the mechanisms involved in this process are largely unknown. Here, we report that microRNA 449c (miR-449c) expression was upregulated in myeloid progenitor cells upon activation of C-X-C motif chemokine receptor 2 (CXCR2) under tumour conditions. MiR-449c upregulation increased the generation of monocytic MDSCs (mo-MDSCs). The increased expression of miR-449c could target STAT6 mRNA in myeloid progenitor cells to shift the differentiation balance of myeloid progenitor cells and lead to an enhancement of the mo-MDSCs population in the tumour environment. Thus, our results demonstrate that the miR-449c/STAT6 axis is involved in the expansion of mo-MDSCs from myeloid progenitor cells upon activation of CXCR2, and thus, inhibition of miR-449c/STAT6 signalling may help to attenuate tumour progression.

Keywords: C-X-C motif chemokine receptor 2, differentiation, microRNA 449c, mo-MDSCs, STAT6

INTRODUCTION

Numerous studies have reported that myeloid-derived suppressor cells (MDSCs) accumulate in the bone marrow, spleen, and blood of patients with different types of cancer and various mouse tumour models (Hoechst et al., 2009; Ko et al., 2009; Ostrand-Rosenberg and Sinha, 2009). MDSCs play an important role in the suppression of T cell immune responses and contribute to tumour growth and metastasis (Wang et al., 2016; Ye et al., 2010). The accumulation of MDSCs under tumour conditions is mediated by various tumour-derived factors, such as interleukin (IL)-10, transforming growth factor-beta (TGF-β), IL-6, and prostaglandin E2 (PGE2) (Chomarat et al., 2000; Goddard et al., 2004; Halliday and Le, 2001; Jing et al., 2003). The increased expression and activity of these tumour-derived factors impairs the normal differentiation of myeloid progenitor cells, which results in the expansion of MDSCs (Gabrilovich et al., 2012).

MDSCs were identified as an immature myeloid heterogeneous population and include polymorphonuclear MDSCs (G-MDSCs), which have a granulocytic phenotype, and mononuclear MDSCs (mo-MDSCs), which have a monocytic phenotype (Movahedi et al., 2008). In mice, G-MDSCs express the Ly6G marker ($CD45^+CD11b^+Ly6C^{low}Ly6G^+$ cells), and mo-MDSCs express the Ly6C marker ($CD45^+CD11b^+Ly6C^+Ly6G^-$ cells) (Gabrilovich et al., 2012). In humans, G-MD-

Received 6 December, 2019; revised 10 August, 2020; accepted 10 August, 2020; published online 31 August, 2020

eISSN: 0219-1032

SCs are $CD14^{-}CD11b^{+}CD33^{+}CD15^{+}$ cells, and mo-MDSCs are $CD14^{+}HLA\text{-}DR^{-}$ or $CD11b^{+}CD14^{-}CD33^{+}CD15^{-}$ cells (Nagaraj and Gabrilovich, 2010). The recruitment of mo-MDSCs to the tumour site serves not only to inhibit the T cell immune response but also to reinforce and maintain a population of hypersuppressive G-MDSCs in the tumour microenvironment (Raber et al., 2014; Youn et al., 2013). However, the molecular mechanisms that regulate the accumulation of mo-MDSCs in tumour conditions remain to be elucidated. Understanding the molecular networks that regulate the expansion of mo-MDSCs is essential to identify potential therapeutic targets for cancer intervention.

MicroRNAs (miRNAs) are a class of endogenous short (approximately 20-25 nt) single-stranded RNAs that bind to the 3′ untranslated region (UTR) of target messenger RNA (mRNA), resulting in cleavage or translational repression (Bartel, 2004). The important role of miRNAs in regulating differentiation, apoptosis, cancer development, and metastasis has been well described (Majumder et al., 2015; Ren et al., 2015; Zang et al., 2015). Some miRNAs cooperate with transcription factors to regulate all aspects of haematopoiesis, including stem cell maintenance, lineage selection, cell expansion, and terminal differentiation (Kim et al., 2019). For instance, miR-129 and miR-520h regulate the differentiation of haematopoietic stem cells into more mature haematopoietic cells (Hong et al., 2015). During mouse lymphocyte differentiation and maturation, miR-150 and miR-146 have been shown to be upregulated (De Tullio et al., 2014; Saki et al., 2015). Some miRNAs have been reported to regulate the accumulation, activation, and immunomodulation of MDSCs in the tumour environment (Chen et al., 2015; El Gazzar, 2014; Wang et al., 2015). However, the regulation of miRNA expression in the tumour environment and the mechanisms by which tumour-derived miRNAs modulate mo-MDSCs expansion and activity remain to be determined.

Here, we profile miRNA expression in C-X-C motif chemokine receptor 2 (CXCR2)-transfected 32D clone 3 cells, which simulate granulocyte and macrophage progenitor cells (GMPs), and show upregulation of microRNA 449c (miR-449c) expression as a characteristic feature of myeloid progenitor cells in response to activation of CXCR2. Using pulldown experiments, we identified STAT6 mRNA as a target of miR-449c in myeloid progenitor cells during differentiation into mo-MDSCs in the tumour environment. Thus, our results demonstrate that the miR-449c/STAT6 axis is involved in CXCR2 activation-induced expansion of mo-MDSCs, suggesting that inhibition of miR-449c/STAT6 signalling may attenuate tumour progression.

MATERIALS AND METHODS

Cell culture

B16F10 cells, HEK-293T cells, and 32D clone 3 cells were purchased from the American Type Culture Collection (ATCC). B16F10 cells and HEK-293T cells were cultured in Dulbecco's modified Eagle's medium (Gibco, USA) supplemented with 10% heat-inactivated foetal bovine serum (Corning, USA). 32D clone 3 cells were maintained in RPMI 1640 medium supplemented with 10% heat-inactivated foetal bovine serum and 10% mouse IL-3 (213-13; PeproTech, USA). B16F10 cells, HEK-293T cells, and 32D clone 3 cells were all cultured with 1% penicillin/streptomycin.

Animal experiments

C57BL/6J mice (female, 8-10 weeks old) used as wild-type (WT) controls were purchased from the Beijing Vital River Laboratory Animal Technology (China). CXCR2-deficient mice on a C57BL/6J background were provided by Dr. Hong Zhou (Department of Immunology, Nanjing Medical University). All mice were housed in a specific pathogen-free environment under protocols approved by the Animal Care Committee of Northeast Normal University, China (NENU/IACUC, AP20160928), and all experiments were performed under the Guidelines for the Care and Use of Laboratory Animals.

In total, 1×10^6 B16F10 cells were subcutaneously injected into the mice. The miR-449c inhibitor was injected into the tail vein of mice with transfection reagent (Entranster^{TM}-in vivo; Engreen Biosystem, China) once a week from the tumour-bearing 1st week to 4th week. Then, the tumour size was measured twice every week from the tumour-bearing 2nd week to 4th week. The tumour volume was calculated using the following formula: $a \times b^2/2$, in which a represents the longest diameter and b represents the shortest diameter.

RNA transcription and real-time polymerase chain reaction (PCR)

Total RNA of bone marrow cells or 32D clone 3 cells was extracted using TRIzol reagent (Invitrogen Life Technologies, USA) according to the manufacturer's instructions. To determine miRNA expression, RNA was subsequently reverse-transcribed using the miRNA 1st Strand cDNA Synthesis Kit (by the stem-loop method) (Vazyme, China) according to the manufacturer's protocol. The primer sequences that were used are listed in Supplementary Table S1. The expression levels of miR-449c and miR-6403 were quantified with SYBR Green Master Mix (Roche, Switzerland) using a miRNA-specific forward primer and a universal poly (T) adaptor reverse primer. The U6 small nuclear RNA was used as an internal reference. To determine mRNA expression, total RNA was reverse transcribed into cDNA according to the manufacturer's instructions (Thermo Fisher Scientific, USA). Real-time PCR was performed on a Roche LightCycler 480 (Roche) real-time RT-PCR system. The primer sequences that were used are listed in Supplementary Table S2.

Construction of the lentiviral expression plasmid and gene transfection

The STAT6 overexpression sequence was cloned into the pWPXLd vector (Addgene, USA), and the constructed plasmid or control plasmid was transfected into HEK-293T cells together with the packaging plasmid psPAX2 (Addgene) and the envelope plasmid pMD2.G (Addgene) using Lipofectamine 2000 reagent (Invitrogen Life Technologies). To overexpress STAT6 in tumour-bearing mice, the collected supernatant was concentrated and intrapleurally injected into two-week tumour-bearing mice four times every other day. To overexpress CXCR2 in 32D clone 3 cells, pEGFP-N1-CXCR2 was electroporated into the cells. The cells were collected by centrifuga-

tion for 5 min at 500*g*, washed once in electroporation buffer (Invitrogen Life Technologies) supplemented with 10% fetal bovine serum without antibiotics, and resuspended in electroporation buffer to a final concentration of 5×10^7 cells/ml. Subsequently, 100 μl of cell suspension was mixed with 4 μg of plasmid DNA in a 0.4 cm^3 gap sterile disposable electroporation cuvette, incubated for 1 min at room temperature and electroporated with an Easyject Plus apparatus (EquiBio, UK). After electroporation, cells were immediately resuspended in fresh complete medium. The related sequences that were used are listed in Supplementary Table S3.

Cell transfection

Transfection of mice bone marrow cells was performed with Lipofectamine 2000 (Invitrogen Life Technologies) according to the manufacturer's instructions. The cells were seeded into 24-well plates at 1×10^6/well. Mimics, inhibitors and negative control (RiboBio, China) of miR-449c were diluted at a working concentration of 20 nM. Mixed diluted transfection agent (Invitrogen Life Technologies) was mixed with diluted mimics, inhibitors or negative control of miR-449c, and then the mixture was incubated at room temperature for 10 min. Then, the transfection complexes were added to the cells, and the medium was changed to fresh complete medium 6 h post transfection. At 24 h post transfection, the cells were used for further experiments. The related sequences that were used are listed in Supplementary Table S4.

Luciferase reporter assay

HEK-293T cells were seeded in 24-well plates overnight in the absence of antibiotics. The cells were then transfected with the STAT6 3′-UTR luciferase reporter plasmid, CEBPα 3′-UTR luciferase reporter plasmid or control vector (pGL3-Control) plus Renilla luciferase reporter plasmid (an internal control; Promega, USA) using Lipofectamine 2000 transfection reagent (Invitrogen Life Technologies). The treated cells were transfected with miR-449c mimic control or miR-449c mimics. To analyse the effects of the 3′-UTR on mRNA levels of target genes, firefly luciferase mRNA levels were measured by quantitative PCR (qPCR) and calibrated to that of Renilla. The related sequences that were used are listed in Supplementary Table S5.

In vitro differentiation experiments

Bone marrow cells were obtained from the femurs of control mice (Chatterjee et al., 2013). The tissues were ground and filtered through a 200 μm cell strainer, and erythrocytes were eliminated using hypotonic lysis buffer (155 mM NH_4Cl, 0.1 mM EDTA, and 10 mM $KHCO_3$). The remaining cells were transfected with miR-449c, then cultured in tumour-conditioned medium supplemented with GM-CSF (10 ng/ml, 315-03; PeproTech) for five days. CXCL1 (50 ng/ml, 250-11; PeproTech) and CXCL2 (50 ng/ml, 250-15; PeproTech) were added to the induction system.

Flow cytometry analysis

Single-cell suspensions of the bone marrow, spleen, and blood samples were prepared and stained as previously described (Shi et al., 2018). The bone marrow and spleen were ground and filtered through a 200 μm cell strainer. To eliminate erythrocytes, a single-cell suspension was treated with hypotonic lysis buffer. The single-cell suspension was stained for 30 min at 4°C with appropriate dilutions of various combinations of the following fluorochrome-conjugated antibodies: anti-CD11b-FITC (clone M1/70), anti-CD45-PE/Cy7 (clone 30-F11), anti-Ly6G-APC/Cy7 (clone 1A8), anti-Ly6C-PE (clone AL-21), anti-CD115-PE/Cy7 (clone AFS98), and anti-CD115-APC (clone AFS98), which were all purchased from BD Biosciences (USA). The cells were further fixed using 10% formaldehyde (Sigma-Aldrich, USA) for 10 min, permeabilized using 0.1% Triton X-100 (Sigma-Aldrich) for 10 min, and then stained for Ki67 (clone 16A8, FITC-conjugated; BioLegend, USA). For the Annexin-V analysis, cells were stained according to the manufacturer's instructions (BD Biosciences). The stained cells were acquired on FACSCanto II (BD Biosciences), and the data were analysed using FACSDiva software (BD Biosciences) and FlowJo 7.6.1 software (Treestar, USA). Dead cells and doublets were excluded based on the forward and side scatter.

Western blot analysis

Harvested cells were washed with phosphate-buffered saline (PBS), and protein was extracted using lysis buffer (150 mM NaCl, 50 mM Tris-HCl [pH 7.5], 1% NP-40, 1 mM EDTA, 0.5% sodium deoxycholate, 0.1% sodium dodecyl sulfate, 1 mM Na_3VO_4, 1 mM NaF, 1 mM PMSF and 0.1 mg/ml leupeptin/aprotinin) on ice for 30 min and centrifuged at 15,000*g* for 30 min. Then, the supernatant was collected for Western blotting. The proteins were separated by sodium dodecyl sulfate-polyacryl amidegel electrophoresis (SDS-PAGE) and transferred onto nitrocellulose blotting membranes (GE Healthcare Life Science, USA). The primary antibodies were incubated with the membrane overnight at 4°C. Horseradish peroxidase-conjugated goat anti-mouse or goat anti-rabbit IgG secondary antibody (Beyotime, China) was incubated with the membranes for 1 h at room temperature. The proteins on the membranes were detected using a Tanon imaging system (5200; Tanon Science & Technology, China). The primary antibodies used included anti-STAT6, anti-CEBPα, anti-CEBPβ, and anti-β-actin, which were all purchased from Cell Signaling Technology (USA).

Cell sorting

To isolate mo-MDSCs, tumour-bearing mice were sacrificed by tail vein injection of 4% EDTA. Blood was collected, and the erythrocytes were eliminated with hypotonic lysis buffer. The remaining cells were collected, and the mo-MDSCs were sorted with a Myeloid-Derived Suppressor Cell Isolation Kit using an AutoMACS sorter (Miltenyi Biotec, Germany) according to the manufacturer's instructions. First, Gr-1^{high} $Ly6G^+$ cells were indirectly magnetically labelled with Anti-Ly6G-Biotin (MDSC-Kit) and Anti-Biotin MicroBeads. Then, the cell suspension was loaded onto a MACS column, which was placed in the magnetic field of a MACS Separator. The magnetically labelled $Ly6G^+$ cells were retained in the column, and the unlabelled cells passed through. The unlabelled cells were depleted of Gr-1^{high} $Ly6G^+$ cells and pre-enriched for Gr-1^{dim} $Ly6G^-$ myeloid cells. The Gr-1^{dim} $Ly6G^-$ myeloid cells

were separated according to Ly6C expression by Aria III (BD Biosciences).

Gene expression analysis

For RNA sequencing (RNA-seq), 32D clone 3 cells transfected with CXCR2 or an empty vector were both incubated with CXCL1 and CXCL2 for 4 h and harvested. Cellular RNA was extracted using TRIzol reagent followed by a genomic DNA elimination step. RNA purity was assessed using the KaiaoK5500® Spectrophotometer (Kaiao, China). The RNA integrity and concentration were assessed using an RNA Nano 6000 Assay Kit with the Bioanalyzer 2100 system (Agilent Technologies, USA). Library construction and sequencing on an Illumina HiSeq 2500 instrument were performed at Annoroad Gene Technology Corporation (China). Bowtie2 v2.2.3 was used to build the genome index, and clean data were then aligned to the reference genome using HISAT2 v2.1.0. The level of gene expression was quantified using a software package called FPKM (fragments per kilobase of transcript per million mapped reads). DEGseq v1.18.0 was used for differential gene expression analysis between two samples with non-biological replicates. MiRNAs with a $\log_2$-fold change > 1 and a P value < 0.05 in RNA sequencing were selected. The RNA-seq raw data and processed expression data for this study have been deposited in the NCBI Gene Expression Omnibus and are accessible through GEO Series accession number: [GEO: GSE140723]. The secure token is elatuammblknjul.

Statistical analysis

All data analyses were performed using IBM SPSS (ver. 22; IBM, USA). Data are presented as the mean ± SD. Student's t-test was used to analyse differences between two groups. One-way ANOVA was used to perform the multi-sample analysis followed by the Tukey post hoc test. Differences at $P < 0.05$ were considered statistically significant (*$P < 0.05$; **$P < 0.01$; ***$P < 0.001$; ns, not significant).

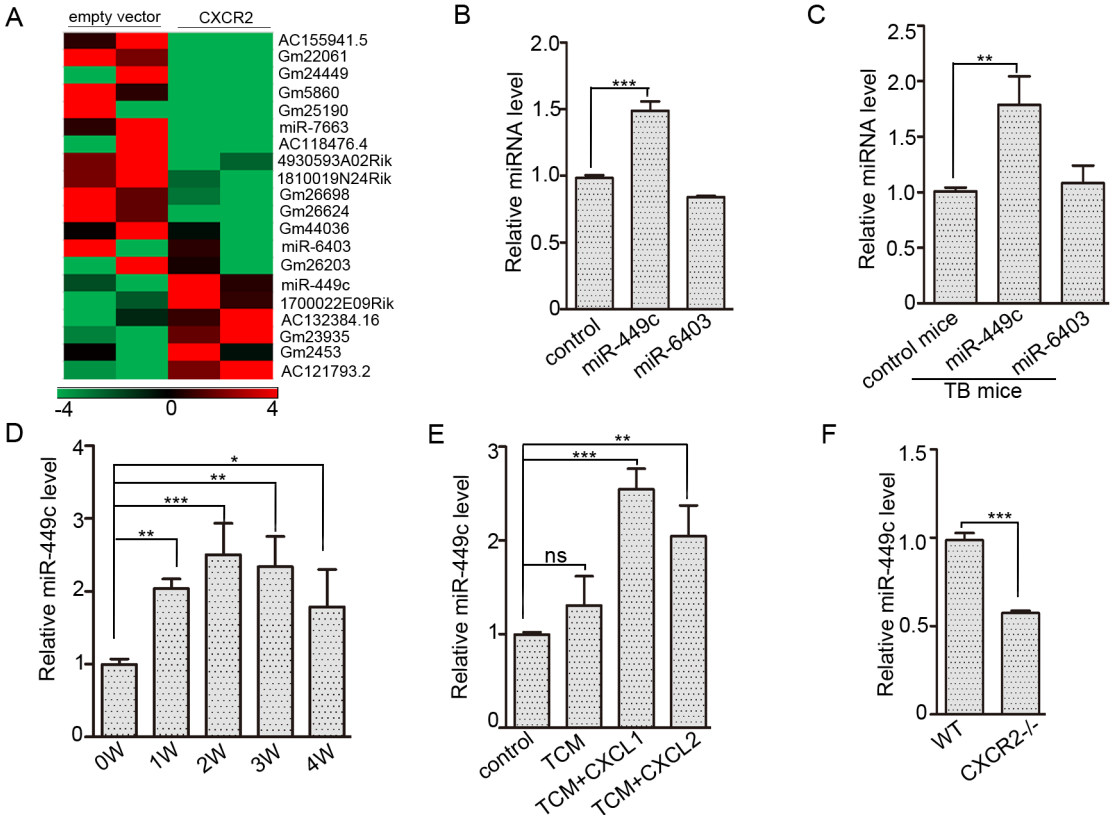

Fig. 1. Activated CXCR2 increases miR-449c expression under tumour conditions. (A) A heat map shows the expression change of non-coding RNA quantified as the $\log_2$-fold change of expression in 32D clone 3 cells. Cells were transfected with CXCR2 or an empty vector and incubated with CXCL1 and CXCL2 for 4 h. (B) The relative expression of miR-449c and miR-6403 in 32D clone 3 cells. 32D clone 3 cells were transfected with CXCR2 or an empty vector and incubated with CXCL1 and CXCL2 for 4 h before qPCR analysis. (C) The relative expression of miR-449c and miR-6403 in bone marrow cells of WT tumour-bearing (TB) mice was analysed by qPCR. (D) The relative expression of miR-449c in bone marrow cells of tumour-bearing mice at 1 week, 2 weeks, 3 weeks, or 4 weeks was analysed by qPCR. (E) The relative expression of miR-449c in bone marrow cells of control mice, which were tail vein injected with PBS, or tumour-conditioned medium (TCM) with or without CXCL1 or CXCL2 four times every other day. The expression of miRNA was analysed by qPCR. (F) The relative expression of miR-449c in bone marrow cells of WT and CXCR2$^{-/-}$ tumour-bearing mice was analysed by qPCR. Bars represent the mean ± SD. *$P < 0.05$; **$P < 0.01$; ***$P < 0.001$; ns, not significant.

RESULTS

MiR-449c expression increases in response to CXCR2 activation

Previous studies have demonstrated that in GMPs, the expression of CXCR2 plays a critical role in the differentiation of haematopoietic progenitor cells into mo-MDSCs under tumour conditions (Han et al., 2019). To elucidate the potential role of non-coding RNA in CXCR2-mediated activation of myeloid progenitor cell differentiation, 32D clone 3 cells were transfected with CXCR2 to simulate GMPs (Supplementary Fig. S1) and examined using RNA sequencing. A $\log_2$-fold change > 3 and a P value < 0.05 were used to identify significant changes in miRNA levels. A downregulation of miR-6403 and an upregulation of miR-449c were observed in 32D clone 3 cells transfected with CXCR2 compared to cells transfected with the empty vector (Fig. 1A). qPCR validation using U6 miRNA as a normalizer also showed an upregulation of miR-449c but did not show significant downregulation of miR-6403 (Fig. 1B). To further validate these results, miR-6403 and miR-449c expression was measured in bone marrow cells of WT tumour-bearing mice, and similar results were obtained (Fig. 1C). MiR-449c expression was examined with the increase in tumour-bearing time. The results showed that miR-449c expression was increased under tumour conditions, with the highest level of expression occurring after 2 weeks of tumour-bearing (Fig. 1D). Next, tumour-conditioned medium with or without CXCL1 or CXCL2 was intravenously injected into normal mice, and miR-449c expression was measured in bone marrow cells. Increased miR-449c expression was observed in bone marrow cells of mice injected with tumour-conditioned medium with CXCL1 or CXCL2 but not in mice injected with tumour-conditioned medium only (Fig. 1E). The expression of miR-449c was also increased in bone marrow cells cultured with CXCL1 or CXCL2 (Supplementary Fig. S2). These results suggest that activated CXCR2 may drive miR-449c expression in bone marrow cells. To further confirm these results, miR-449c expression was mea-

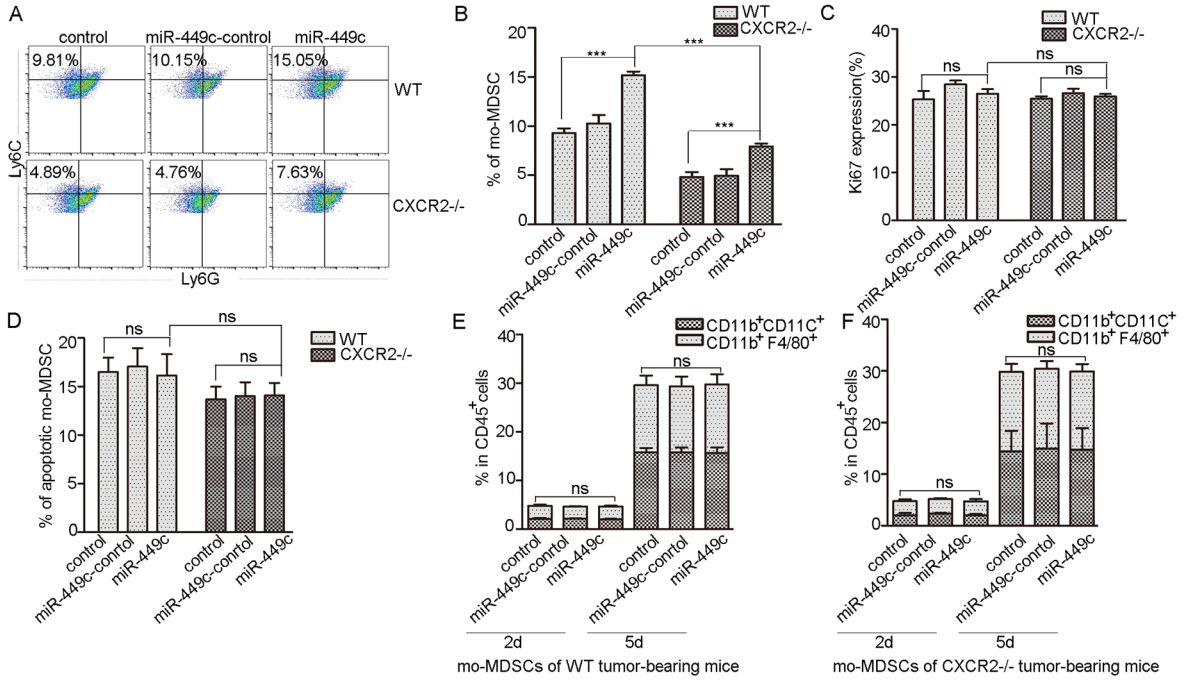

Fig. 2. MiR-449c overexpression increases the differentiation of bone marrow cells to mo-MDSCs. (A) The percentage of mo-MDSCs in WT or CXCR2$^{-/-}$ bone marrow cells was detected by flow cytometry. The bone marrow cells were transfected with a miR-449c mimic or a miR-449c mimic control and cultured in tumour-conditioned medium with CXCL1, CXCL2, and GM-CSF for 5 days. (B) Quantitative analyses of the percentage of mo-MDSCs as shown in Fig. 2A. (C) The expression of Ki67 in mo-MDSCs induced from bone marrow cells of WT or CXCR2$^{-/-}$ control mice was analysed by flow cytometry. Bone marrow cells were transfected with a miR-449c mimic and a miR-449c mimic control, and the treated cells were cultured in tumour-conditioned medium with CXCL1, CXCL2, and GM-CSF for five days. (D) Annexin V expression in mo-MDSCs induced from bone marrow cells of WT or CXCR2$^{-/-}$ control mice was analysed by flow cytometry. Bone marrow cells were transfected with a miR-449c mimic or a miR-449c mimic control, and the treated cells were cultured in tumour-conditioned medium with CXCL1, CXCL2 and GM-CSF for five days. (E) Differentiation of mo-MDSCs into CD11b^{+}CD11c^{+} and CD11b^{+} F4/80^{+} cells was analysed by flow cytometry. The mo-MDSCs were transfected with a miR-449c mimic or a miR-449c mimic control. Treated cells were cultured with GM-CSF for 2 or 5 days. The mo-MDSCs were isolated from the blood of WT tumour-bearing mice. (F) Differentiation of mo-MDSCs into CD11b^{+}CD11c^{+} and CD11b^{+} F4/80^{+} cells was analysed by flow cytometry. The mo-MDSCs were transfected with a miR-449c mimic or a miR-449c mimic control. Treated cells were cultured with GM-CSF for 2 or 5 days. The mo-MDSCs were isolated from the blood of CXCR2$^{-/-}$ tumour-bearing mice. Bars represent the mean ± SD. ***P < 0.001; ns, not significant.

sured in bone marrow cells of WT and CXCR2$^{-/-}$ tumour-bearing mice. The results showed lower miR-449c expression in CXCR2$^{-/-}$ tumour-bearing mice than in WT tumour-bearing mice (Fig. 1F). Therefore, we focused our subsequent efforts on understanding the consequences and mechanisms of miR-449c upregulation in CXCR2 activation-induced generation of mo-MDSCs under tumour conditions.

MiR-449c overexpression increases the generation of mo-MDSCs

To investigate whether miR-449c is related to CXCR2-mediated differentiation of haematopoietic progenitor cells, bone marrow cells of WT or CXCR2$^{-/-}$ control mice were transfected with a miR-449c mimic (Supplementary Fig. S3) and cultured in the presence of CXCL1 and CXCL2. Overexpression of miR-449c significantly increased the percentage of mo-MDSCs in bone marrow cells of both WT and CXCR2$^{-/-}$ control mice. The transfection of the miR-449c mimic in bone marrow cells of CXCR2$^{-/-}$ control mice did not enhance the percentage of mo-MDSCs to the extent that was observed in the bone marrow cells of WT control mice (Figs. 2A and 2B). Overexpression of miR-449c had no effect on the suppressive activity of mo-MDSCs from WT compared to CXCR2$^{-/-}$ mice (Supplementary Fig. S4). These data suggest that miR-449c overexpression increased the accumulation of mo-MDSCs and that the increase was correlated with CXCR2 activation. The overexpression of miR-449c did not affect the proliferation and apoptosis of mo-MDSCs induced from WT or CXCR2$^{-/-}$ bone marrow cells (Figs. 2C and 2D). Upon appropriate stimulation, mo-MDSCs have been shown to differentiate into dendritic cells (CD11b^{+}CD11c^{+}) and macrophages (CD11b^{+}F4/80^{+}) (Poh et al., 2009), therefore, mo-MDSC differentiation was examined. The data showed that there were no significant differences in the percentage of dendritic cells or macrophages derived from mo-MDSCs sorting from WT compared to CXCR2$^{-/-}$ tumour-bearing mice (Supplementary Fig. S5). Next, mo-MDSCs were sorted from the blood of WT or CXCR2$^{-/-}$ tumour-bearing mice, miR-449c was overexpressed in these cells, and the percentage of dendritic cells or macrophages derived from mo-MDSCs was examined. The results showed that miR-449c overexpression did not influence the ability of mo-MDSCs to differentiate into dendritic cells or macrophages (Figs. 2E and 2F). Taken together, these results indicate that miR-449c overexpression promotes the differentiation of myeloid progenitor cells to mo-MDSCs under tumour conditions.

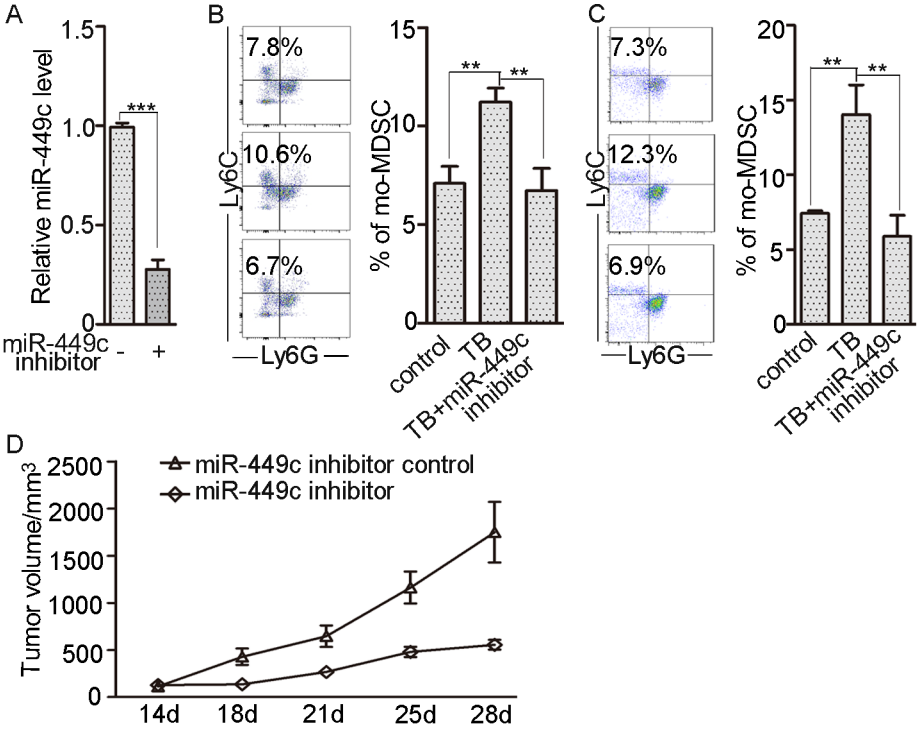

Fig. 3. MiR-449c promotes tumour progression by increasing the accumulation of mo-MDSCs. (A) The relative expression of miR-449c in bone marrow cells of WT tumour-bearing (TB) mice was analysed by qPCR. The mice were injected with or without a miR-449c inhibitor via the tail vein. (B) The percentage of mo-MDSCs in the bone marrow was analysed by flow cytometry. Mice were treated as described in Fig. 3A. TB group means that WT tumour-bearing mice were injected with PBS and TB+miR-449c inhibitor group means that WT tumour-bearing mice were injected with a miR-449c inhibitor. (C) The percentage of mo-MDSCs in the blood was analysed by flow cytometry. The mice were treated as described in Fig. 3A. TB group means that WT tumour-bearing mice were injected with PBS and TB+miR-449c inhibitor group means that WT tumour-bearing mice were injected with a miR-449c inhibitor. (D) B16F10 cells were subcutaneously inoculated into mice, and tumour size was measured at the indicated time points. The mice were treated as described in Fig. 3A. Bars represent the mean ± SD. $^{**}P < 0.01$; $^{***}P < 0.001$.

MiR-449c promotes tumour progression by increasing the generation of mo-MDSCs

To determine whether increased mo-MDSCs generation resulting from upregulation of miR-449c under tumour conditions contributes to tumour progression, a miR-449c inhibitor was injected into WT tumour-bearing mice via the tail vein once a week during tumour-bearing weeks one through four. The results showed that miR-449 expression was inhibited in bone marrow cells (Fig. 3A), and the miR-449c inhibitor decreased the percentage of mo-MDSCs in the bone marrow and blood of tumour-bearing mice (Figs. 3B and 3C). Furthermore, a significant inhibition of melanoma growth was observed in miR-449c inhibitor-injected mice compared with untreated mice after 2 weeks of tumour bearing (Fig. 3D). These results suggest that miR-449c promotes tumour progression by increasing the accumulation of mo-MDSCs.

STAT6 is a direct target of miR-449c

Our data thus far demonstrate that miR-449c expression is increased in bone marrow cells upon CXCR2 activation, but the molecular mechanisms underlying these functions require further exploration. Some transcription factors, such as CEBPα, CEBPβ, and STAT6, are important for the differentiation of myeloid progenitor cells (Friedman, 2015; Marigo et al., 2010; Munera et al., 2010); therefore, we hypothesized that miR-449c promotes the accumulation of mo-MDSCs by targeting these transcription factors. To test this hypothesis, miR-449c was overexpressed in bone marrow cells. Overexpression of miR-449c resulted in a decrease in CEBPα, CEBPβ, and STAT6 mRNA expression in bone marrow cells (Fig. 4A). CEBPα and STAT6 protein expression was decreased in bone marrow cells with miR-449c overexpression and increased upon inhibition of miR-449c expression (Figs. 4B and 4C). In contrast, CEBPβ protein expression in bone marrow cells was not dramatically changed upon increasing or inhibiting miR-449c expression (Figs. 4B and 4C). These results suggest that miR-449c may target CEBPα and STAT6 to regulate the accumulation of mo-MDSCs. An online bioinformatics database (TargetScan; http://www.targetscan.org/vert_71/) was used to identify putative targets of miR-449c in bone marrow cells. Based on the predictions from TargetScan, the 3′-UTR of the STAT6 gene was revealed to contain the binding sequences of miR-449c, whereas the 3′-UTR of the CEBPα gene was not predicted to contain the binding sequences, suggesting that STAT6 may be a downstream target of miR-449c (Fig. 4D). To determine whether miR-449c can interact with the STAT6 3′-UTR or CEBPα 3′-UTR, luciferase assays were performed. Overexpression of miR-449c in bone marrow cells significantly reduced luciferase mRNA levels of the STAT6 3′-UTR but had no effect on that of the control vector or CEBPα 3′-UTR (Fig. 4E). The modulation of STAT6 expression and STAT6-targeted gene expression (*Arg1* and *TGF-beta*) were similar after treatment with miR-449c mimic or inhibitor (Supplementary Fig. S6). The results indicate that miR-449c interacts with the STAT6 3′-UTR in bone marrow cells when CXCR2 is activated.

Overexpression of miR-449c blocks the inhibitory effect of STAT6 on the generation of mo-MDSCs

Immunoblot analyses showed that the expression of STAT6 was increased in bone marrow cells of tumour-bearing mice, and this increase was further enhanced in mice after intrapleural injection with a lentivirus-based STAT6 overexpression sequence (Fig. 5A). The percentage of mo-MDSCs and G-MDSCs was analysed, and the results showed that the percentage of mo-MDSCs was decreased in the bone marrow, spleen, and blood of the tumour-bearing mice with STAT6 overexpression (Fig. 5B, Supplementary Fig. S7). The percentage of G-MDSCs was increased in the bone marrow and blood but was decreased in the spleen of tumour-bearing mice overexpressing STAT6 (Fig. 5C, Supplementary Fig. S7). To further confirm whether STAT6 is the mediator of the biological function of miR-449c in bone marrow cells, cells from WT control mice were transfected with STAT6, the miR-449c mimic and STAT6, or the miR-449c mimic control and STAT6. The results of immunoblot analyses showed that miR-449c overexpression inhibited STAT6 expression (Fig. 5D). The percentage of mo-MDSCs and G-MDSCs that were derived from the transfected cells was examined. The results showed that STAT6 overexpression decreased the percentage of mo-MDSCs and increased the percentage of G-MDSCs. In contrast, the opposite results were found in the group of cells transfected with the miR-449c mimic and STAT6. This was because the expression of STAT6 was inhibited by miR-449c overexpression (Figs. 5E and 5F, Supplementary Fig. S8). These data suggest that overexpression of miR-449c decreases the inhibitory effect of STAT6 on the generation of mo-MDSCs.

DISCUSSION

Several studies have identified miR449c as a novel cancer-related miRNA and an important regulator of proliferation and invasion in nonsmall cell lung cancer and gastric cancer (Chen et al., 2018; Miao et al., 2013). In liver cancer, miR449c acts as a tumour suppressor by promoting cell death and inhibiting cell migration (Sandbothe et al., 2017). Furthermore, miR449c belongs to the family of miRNAs that plays an essential role in regulating brain development, motile ciliogenesis, and spermatogenesis (Wu et al., 2014). The present study demonstrated that miR-449c was upregulated in myeloid progenitor cells of WT tumour-bearing mice compared with $CXCR2^{-/-}$ tumour-bearing mice (Fig. 1F), suggesting that miR-449c expression was dependent upon activation of CXCR2 under tumour conditions. CXCR2 activation-mediated expression of miR-449c was found to be highest in bone marrow cells at 2 weeks of tumour-bearing (Fig. 1D), and the percentage of mo-MDSCs in the bone marrow was increased in tumour-bearing mice at 3 weeks (Han et al., 2019). These data indicate that increased miR-449c expression may be a necessary event for the expansion of mo-MDSCs.

It has been reported that miR-449c is downregulated in several tumour tissues (Chen et al., 2018; Miao et al., 2013), but the mechanism underlying this downregulation remains largely unknown. The results presented here demonstrate that the upregulated expression of miR-449c in bone marrow

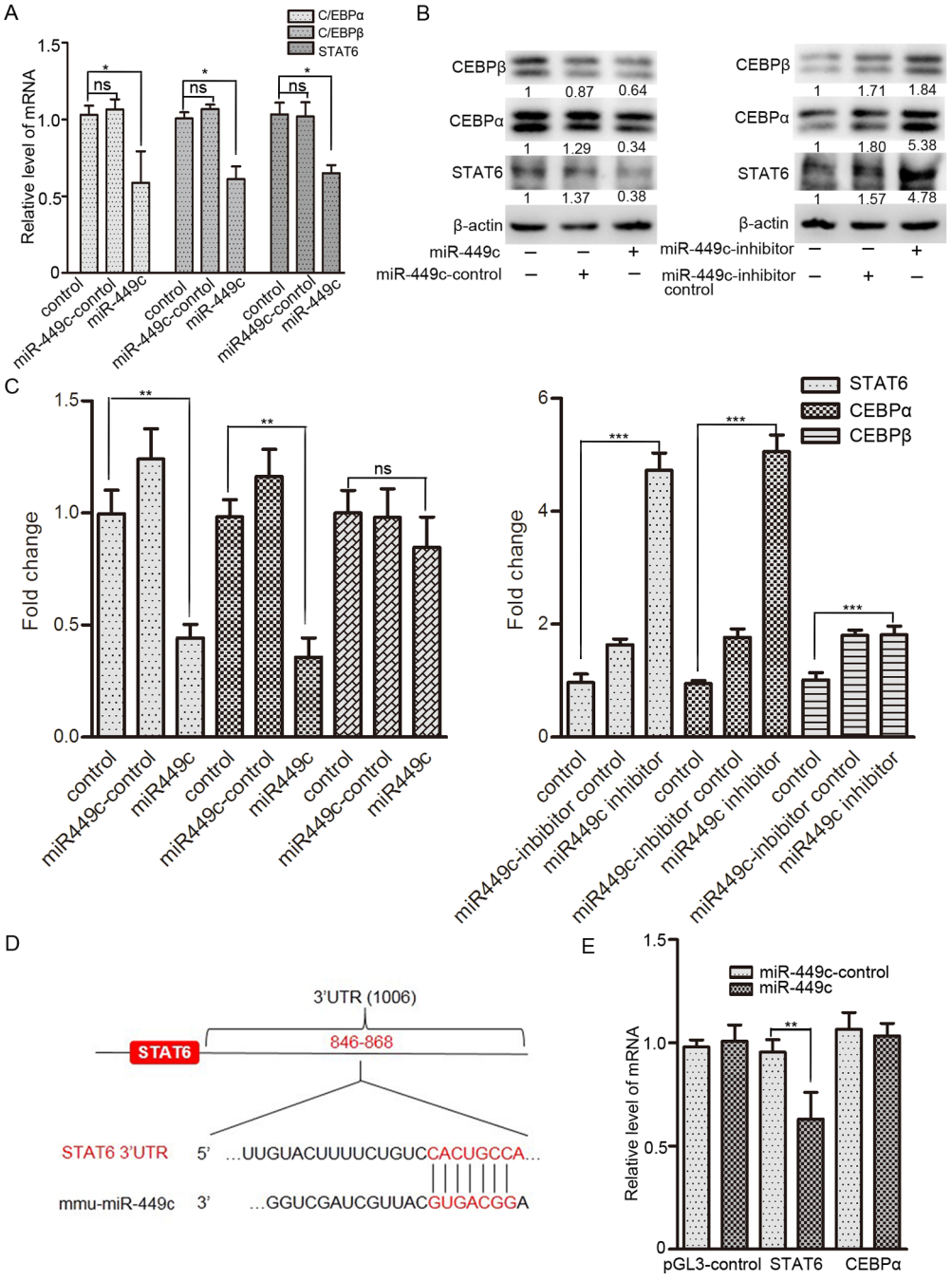

Fig. 4. STAT6 is a direct target of miR-449c. (A) The relative mRNA expression levels of *CEBPα*, *CEBPβ*, and *STAT6* were analysed in bone marrow cells by qPCR. The bone marrow cells of WT control mice were transfected with a miR-449c mimic or a miR-449c mimic control and cultured in tumour-conditioned medium in the presence of CXCL1, CXCL2, and GM-CSF for 5 days. (B) The expression of CEBPα, CEBPβ, and STAT6 in bone marrow cells was analysed by Western blotting. The bone marrow cells of WT control mice were transfected with a miR-449c mimic, a miR-449c mimic control, a miR-449c inhibitor or a miR-449c inhibitor control and cultured in tumour-conditioned medium in the presence of CXCL1, CXCL2, and GM-CSF for 5 days. (C) Quantitative analyses of the protein levels in Fig. 4B were conducted by ImageJ software. CEBPα, CEBPβ, and STAT6 were normalized to β-actin. (D) The predicted binding sites of miR-449c in the STAT6 3′-UTR. (E) The mRNA levels of luciferase in HEK-293T cells were analysed by qPCR. HEK-293T cells were transfected with reporter plasmids containing STAT6 3′-UTR, CEBPα 3′-UTR, or vector pGL3-control plus a Renilla reporter plasmid and transfected with a miR-449c mimic control or a miR-449c mimic. Bars represent the mean ± SD. $*P < 0.05$; $**P < 0.01$; $***P < 0.001$; ns, not significant.

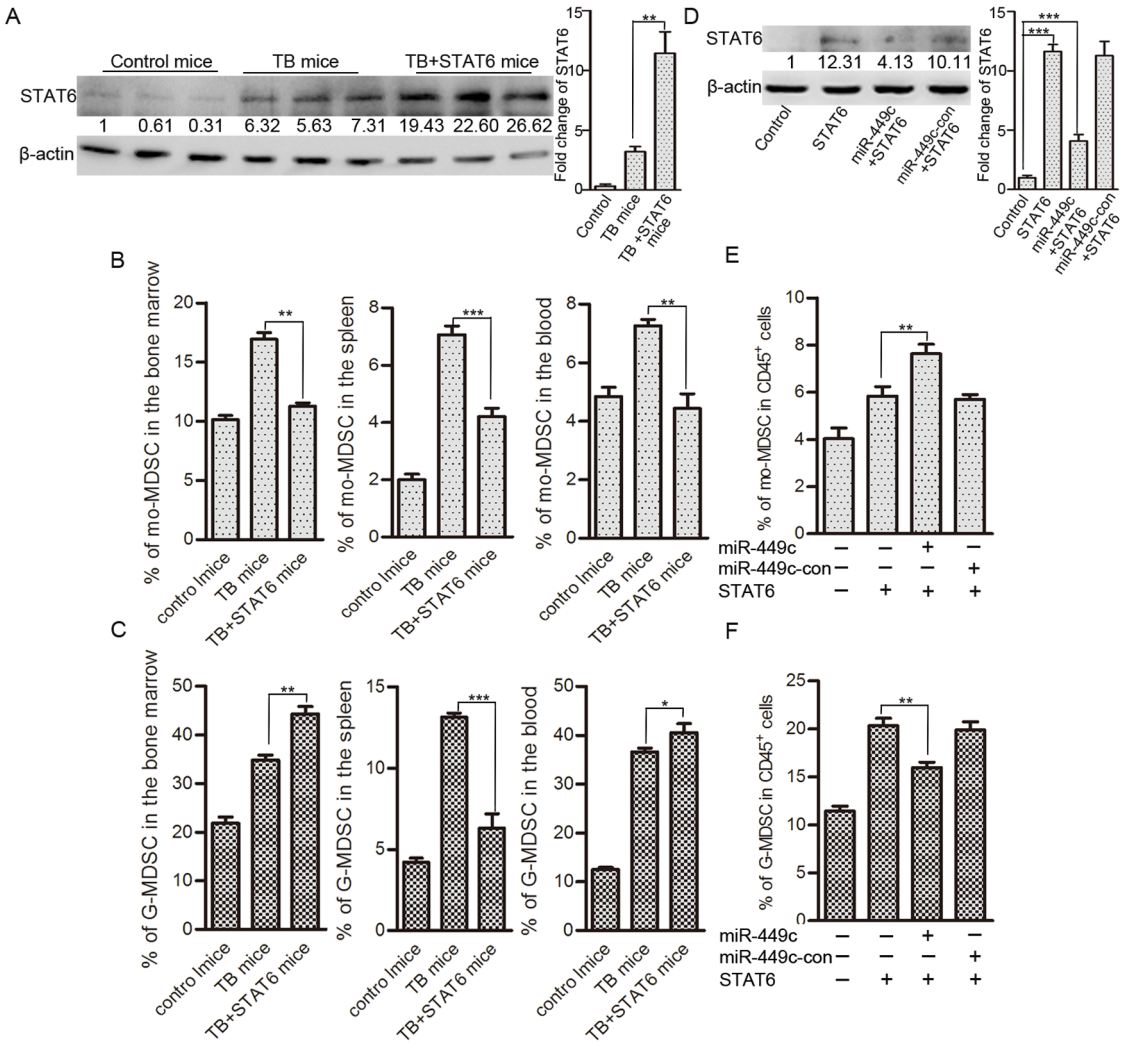

Fig. 5. Overexpression of miR-449c blocks the inhibitory effect of STAT6 on the generation of mo-MDSCs. (A) The expression of STAT6 in bone marrow cells of control mice, WT tumour-bearing (TB) mice, or WT tumour-bearing mice intrapleurally injected with a lentivirus-based STAT6 overexpression sequence was analysed by Western blotting. Quantitative analyses of the proteins were conducted by ImageJ software. STAT6 was normalized to β-actin. (B) The percentages of mo-MDSCs in the bone marrow, spleen, and blood were quantitatively analysed by flow cytometry. Mice were treated as described in Fig. 5A. (C) Quantitative analyses of the percentages of G-MDSCs in the bone marrow, spleen, and blood were conducted by flow cytometry. Mice were treated as described in Fig. 5A. (D) The expression of STAT6 in bone marrow cells of WT control mice. The bone marrow cells were transfected with STAT6, a miR-449c mimic and STAT6, or a miR-449c mimic control and STAT6 and cultured in tumour-conditioned medium with CXCL1 and CXCL2 for 24 h. Quantitative analyses of the proteins were conducted by ImageJ software. STAT6 was normalized to β-actin. (E and F) The percentage of mo-MDSCs and G-MDSCs was examined by flow cytometry. Bone marrow cells were transfected with STAT6, a miR-449c mimic and STAT6, or a miR-449c mimic control and STAT6. Then, the treated cells were cultured in tumour-conditioned medium in the presence of CXCL1, CXCL2, and GM-CSF for 4 days. Bars represent the mean ± SD. $*P < 0.05$; $**P < 0.01$; $***P < 0.001$.

is a result of CXCR2 activation in myeloid progenitor cells, suggesting that miR-449c may play a cell type-specific role across different tissues.

We also reported a novel discovery that STAT6 is a downstream target of miR-449c in myeloid progenitor cells. We showed that STAT6 promotes the expansion of G-MDSCs, but weakens the expansion of mo-MDSCs in a subcutaneous model of melanoma (Figs. 5B and 5C). In contrast, STAT6 has been previously reported to promote the expansion of G-MDSCs and mo-MDSCs in a colorectal cancer model (Jayakumar and Bothwell, 2017; Leon-Cabrera et al., 2017). The different effects of STAT6 on the expansion of mo-MDSCs may be caused by the differences in tumour heterogeneity. Moreover, we increased the expression of STAT6 in mice by intrapleural injection with a lentivirus-based STAT6 overexpression sequence. Knocking down STAT6 may have a wider impact than overexpressing STAT6 in mice. MiR-449c overexpression blocks the inhibitory effect of STAT6 on the expan-

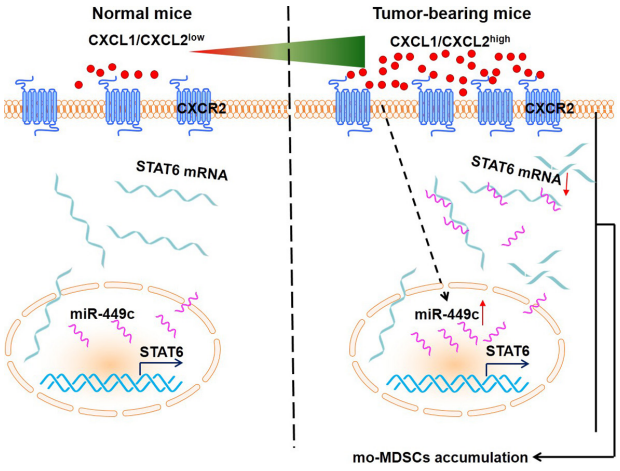

Fig. 6. Schematic illustration of the proposed model. The levels of CXCL1 and CXCL2 are very low under normal physiological conditions, but the levels are greatly increased under tumour conditions. The increased CXCL1 and CXCL2 bind to its receptor CXCR2 on myeloid progenitor cells. In this case, the level of miR-449c in myeloid progenitor cells is increased, and miR-449c enhances the generation of mo-MDSCs by targeting and suppressing STAT6 mRNA.

sion of mo-MDSCs (Figs. 5E and 5F). These data suggest that miR-449c may weaken the STAT6-mediated inhibition of the differentiation of myeloid progenitor cell to mo-MDSCs under tumour conditions. It is important to note that the STAT6 pathway was originally reported to regulate the survival and accumulation of MDSCs via CD124 (Roth et al., 2012), and was also shown to mediate MDSC suppression by increasing the activity of arginase-1 (Condamine et al., 2015). Thus, our study serves to further understand the role of the STAT6 pathway in the accumulation of MDSCs. A previous study showed that CXCR2 regulates the differentiation of GMPs into mo-MDSCs through the ERK/STAT3 pathway (Han et al., 2019). Therefore, our results suggest that the STAT family of transcription factors performs a different function in the accumulation of mo-MDSCs and G-MDSCs.

In summary, the present study demonstrated that miR-449c expression was upregulated in myeloid progenitor cells in response to CXCR2 activation. The increased expression of miR449c was associated with the generation of mo-MDSCs. Overexpression of miR449c contributed to the expansion of mo-MDSCs, whereas knockdown of miR449c expression inhibited differentiation of myeloid progenitor cells to mo-MDSCs. Finally, STAT6 was identified as a novel downstream target and functional mediator of miR449c during the differentiation of myeloid progenitor cells (Fig. 6).

Note: Supplementary information is available on the Molecules and Cells website (www.molcells.org).

ACKNOWLEDGMENTS

We thank Dr. Hong Zhou (Department of Immunology, Nanjing Medical University) for the support with C57BL/6J CXCR2$^{-/-}$ mice. This work was funded by The National Nature Science Foundation of China. The grant numbers are 81670095, 31870888, and 81372288.

AUTHOR CONTRIBUTIONS

X.H. and T.L. performed experiments. X.H., T.L., Y.S., W.Y., and D.W. analyzed the data. X.Z. supervised the research. X.H. and X.Z. wrote the manuscript. All authors read and approved the manuscript.

CONFLICT OF INTEREST

The authors have no potential conflicts of interest to disclose.

ORCID

Xiaoqing Han https://orcid.org/0000-0003-4722-9083
Tao Luan https://orcid.org/0000-0001-9560-9764
Yingying Sun https://orcid.org/0000-0003-2751-7133
Wenyi Yan https://orcid.org/0000-0001-9006-6270
Dake Wang https://orcid.org/0000-0002-7834-3869
Xianlu Zeng https://orcid.org/0000-0002-2655-4197

REFERENCES

Bartel, D.P. (2004). MicroRNAs: genomics, biogenesis, mechanism, and function. Cell *116*, 281-297.

Chatterjee, S., Das, S., Chakraborty, P., Manna, A., Chatterjee, M., and Choudhuri, S.K. (2013). Myeloid derived suppressor cells (MDSCs) can induce the generation of Th17 response from naive CD4+ T cells. Immunobiology *218*, 718-724.

Chen, S., Zhang, Y., Kuzel, T.M., and Zhang, B. (2015). Regulating tumor myeloid-derived suppressor cells by microRNAs. Cancer Cell Microenviron. *2*, e637.

Chen, X., Wang, A., and Yue, X. (2018). miR-449c inhibits migration and invasion of gastric cancer cells by targeting PFKFB3. Oncol. Lett. *16*, 417-424.

Chomarat, P., Banchereau, J., Davoust, J., and Palucka, A.K. (2000). IL-6 switches the differentiation of monocytes from dendritic cells to macrophages. Nat. Immunol. *1*, 510-514.

Condamine, T., Mastio, J., and Gabrilovich, D.I. (2015). Transcriptional regulation of myeloid-derived suppressor cells. J. Leukoc. Biol. *98*, 913-922.

De Tullio, G., De Fazio, V., Sgherza, N., Minoia, C., Serrati, S., Merchionne, F., Loseto, G., Iacobazzi, A., Rana, A., Petrillo, P., et al. (2014). Challenges and opportunities of microRNAs in lymphomas. Molecules *19*, 14723-14781.

El Gazzar, M. (2014). microRNAs as potential regulators of myeloid-derived suppressor cell expansion. Innate Immun. *20*, 227-238.

Friedman, A.D. (2015). C/EBPalpha in normal and malignant myelopoiesis. Int. J. Hematol. *101*, 330-341.

Gabrilovich, D.I., Ostrand-Rosenberg, S., and Bronte, V. (2012). Coordinated regulation of myeloid cells by tumours. Nat. Rev. Immunol. *12*, 253-268.

Goddard, S., Youster, J., Morgan, E., and Adams, D.H. (2004). Interleukin-10 secretion differentiates dendritic cells from human liver and skin. Am. J. Pathol. *164*, 511-519.

Halliday, G.M. and Le, S. (2001). Transforming growth factor-beta produced by progressor tumors inhibits, while IL-10 produced by regressor tumors enhances, Langerhans cell migration from skin. Int. Immunol. *13*, 1147-1154.

Han, X., Shi, H., Sun, Y., Shang, C., Luan, T., Wang, D., Ba, X., and Zeng, X. (2019). CXCR2 expression on granulocyte and macrophage progenitors under tumor conditions contributes to mo-MDSC generation via SAP18/ERK/STAT3. Cell Death Dis. *10*, 598.

Hoechst, B., Voigtlaender, T., Ormandy, L., Gamrekelashvili, J., Zhao, F., Wedemeyer, H., Lehner, F., Manns, M.P., Greten, T.F., and Korangy, F. (2009). Myeloid derived suppressor cells inhibit natural killer cells in patients with hepatocellular carcinoma via the NKp30 receptor. Hepatology *50*, 799-807.

Hong, S.H., Kim, K.S., and Oh, I.H. (2015). Concise review: exploring miRNAs--toward a better understanding of hematopoiesis. Stem Cells *33*, 1-7.

Jayakumar, A. and Bothwell, A. (2017). Stat6 promotes intestinal tumorigenesis in a mouse model of adenomatous polyposis by expansion of MDSCs and inhibition of cytotoxic CD8 response. Neoplasia *19*, 595-605.

Jing, H., Vassiliou, E., and Ganea, D. (2003). Prostaglandin E2 inhibits production of the inflammatory chemokines CCL3 and CCL4 in dendritic cells. J. Leukoc. Biol. *74*, 868-879.

Kim, M., Civin, C.I., and Kingsbury, T.J. (2019). MicroRNAs as regulators and effectors of hematopoietic transcription factors. Wiley Interdiscip. Rev. RNA *10*, e1537.

Ko, J.S., Zea, A.H., Rini, B.I., Ireland, J.L., Elson, P., Cohen, P., Golshayan, A., Rayman, P.A., Wood, L., Garciaet, L., et al. (2009). Sunitinib mediates reversal of myeloid-derived suppressor cell accumulation in renal cell carcinoma patients. Clin. Cancer Res. *15*, 2148-2157.

Leon-Cabrera, S.A., Molina-Guzman, E., Delgado-Ramirez, Y.G., Vázquez-Sandoval, A., Ledesma-Soto, Y., Pérez-Plasencia, C.G., Chirino, Y.I., Delgado-Buenrostro, N.L., Rodríguez-Sosa, M., Vaca-Paniagua, F., et al. (2017). Lack of STAT6 attenuates inflammation and drives protection against early steps of colitis-associated colon cancer. Cancer Immunol. Res. *5*, 385-396.

Majumder, M., Landman, E., Liu, L., Hess, D., and Lala, P.K. (2015). COX-2 elevates oncogenic miR-526b in breast cancer by EP4 activation. Mol. Cancer Res. *13*, 1022-1033.

Marigo, I., Bosio, E., Solito, S., Mesa, C., Fernandez, A., Dolcetti, L., Ugel, S., Sonda, N., Bicciato, S., Falisi, E., et al. (2010). Tumor-induced tolerance and immune suppression depend on the C/EBPbeta transcription factor. Immunity *32*, 790-802.

Miao, L.J., Huang, S.F., Sun, Z.T., Gao, Z.Y., Zhang, R.X., Liu, Y., and Wang, J. (2013). MiR-449c targets c-Myc and inhibits NSCLC cell progression. FEBS Lett. *587*, 1359-1365.

Movahedi, K., Guilliams, M., Van den Bossche, J., Van den Bergh, R., Gysemans, C., Beschin, A., Baetselier, P.D., and Ginderachter J.A. (2008). Identification of discrete tumor-induced myeloid-derived suppressor cell subpopulations with distinct T cell-suppressive activity. Blood *111*, 4233-4244.

Munera, V., Popovic, P.J., Bryk, J., Pribis, J., Caba, D., Matta, B.M., Zenati, M., and Ochoa, J.B. (2010). Stat 6-dependent induction of myeloid derived suppressor cells after physical injury regulates nitric oxide response to endotoxin. Ann. Surg. *251*, 120-126.

Nagaraj, S. and Gabrilovich, D.I. (2010). Myeloid-derived suppressor cells in human cancer. Cancer J. *16*, 348-353.

Ostrand-Rosenberg, S. and Sinha, P. (2009). Myeloid-derived suppressor cells: linking inflammation and cancer. J. Immunol. *182*, 4499-4506.

Poh, T.W., Bradley, J.M., Mukherjee, P., and Gendler, S.J. (2009). Lack of Muc1-regulated beta-catenin stability results in aberrant expansion of CD11b+Gr1+ myeloid-derived suppressor cells from the bone marrow. Cancer Res. *69*, 3554-3562.

Raber, P.L., Thevenot, P., Sierra, R., Wyczechowska, D., Halle, D., Cheng, P.Y., Villagra, A., Antonia, S., McCaffrey, J.C., Fishman, M., et al. (2014). Subpopulations of myeloid-derived suppressor cells impair T cell responses through independent nitric oxide-related pathways. Int. J. Cancer *134*, 2853-2864.

Ren, X., Bai, X., Zhang, X., Li, Z., Tang, L., Zhao, Y.X., Li, Z.Y., Ren, Y.F., Wei, S.C., Wang, Q.S., et al. (2015). Quantitative nuclear proteomics identifies that miR-137-mediated EZH2 reduction regulates resveratrol-induced apoptosis of neuroblastoma cells. Mol. Cell. Proteomics *14*, 316-328.

Roth, F., De La Fuente, A.C., Vella, J.L., Zoso, A., Inverardi, L., and Serafini, P. (2012). Aptamer-mediated blockade of IL4Ralpha triggers apoptosis of MDSCs and limits tumor progression. Cancer Res. *72*, 1373-1383.

Saki, N., Abroun, S., Soleimani, M., Hajizamani, S., Shahjahani, M., Kast, R.E., and Mortazavi, Y. (2015). Involvement of microRNA in T-cell differentiation and malignancy. Int. J. Hematol. Oncol. Stem Cell Res. *9*, 33-49.

Sandbothe, M., Buurman, R., Reich, N., Greiwe, L., Vajen B., Gürlevik, E., Schäffer, V., Eilers, M., Kühnel, F., Vaquero, A., et al. (2017). The microRNA-449 family inhibits TGF-beta-mediated liver cancer cell migration by targeting SOX4. J. Hepatol. *66*, 1012-1021.

Shi, H., Han, X., Sun, Y., Shang, C., Wei, M., Ba, X., and Zeng, X. (2018). Chemokine (C-X-C motif) ligand 1 and CXCL2 produced by tumor promote the generation of monocytic myeloid-derived suppressor cells. Cancer Sci. *109*, 3826-3839.

Wang, J., De Veirman, K., De Beule, N., Maes, K., De Bruyne, E., Vanderkerken, K., and Menu, E. (2015). The bone marrow microenvironment enhances multiple myeloma progression by exosome-mediated activation of myeloid-derived suppressor cells. Oncotarget *6*, 43992-44004.

Wang, J., Su, X., Yang, L., Qiao, F., Fang, Y., Fang, F., Yu, L., Yang, Q., Wang, Y.Y., Yin, Y.F., et al. (2016). The influence of myeloid-derived suppressor cells on angiogenesis and tumor growth after cancer surgery. Int. J. Cancer *138*, 2688-2699.

Wu, J., Bao, J., Kim, M., Yuan, S., Tang, C., Zheng, H., Mastick, G.S., Xu, C., and Yan, W. (2014). Two miRNA clusters, miR-34b/c and miR-449, are essential for normal brain development, motile ciliogenesis, and spermatogenesis. Proc. Natl. Acad. Sci. U. S. A. *111*, E2851-E2857.

Ye, X.Z., Yu, S.C., and Bian, X.W. (2010). Contribution of myeloid-derived suppressor cells to tumor-induced immune suppression, angiogenesis, invasion and metastasis. J. Genet. Genomics *37*, 423-430.

Youn, J.I., Kumar, V., Collazo, M., Nefedova, Y., Condamine, T., Cheng, P., Villagra, A., Antonia, S., McCaffrey, J.C., Fishmanet, M., et al. (2013). Epigenetic silencing of retinoblastoma gene regulates pathologic differentiation of myeloid cells in cancer. Nat. Immunol. *14*, 211-220.

Zang, W., Wang, Y., Wang, T., Du, Y., Chen, X., Li, M., and Zhao, G.Q. (2015). miR-663 attenuates tumor growth and invasiveness by targeting eEF1A2 in pancreatic cancer. Mol. Cancer *14*, 37.